

Studies of GaP:V by thermally detected electron paramagnetic resonance and optical absorption: The V^{2+} problem

This article has been downloaded from IOPscience. Please scroll down to see the full text article.

1993 J. Phys.: Condens. Matter 5 7669

(<http://iopscience.iop.org/0953-8984/5/41/015>)

View [the table of contents for this issue](#), or go to the [journal homepage](#) for more

Download details:

IP Address: 171.66.16.96

The article was downloaded on 11/05/2010 at 02:01

Please note that [terms and conditions apply](#).

Studies of GaP:V by thermally detected electron paramagnetic resonance and optical absorption: the V^{2+} problem

A-M Vasson†||, A Vasson†||, A Gavaix†||, N Tebbal†, M En-Naqadi†, A Erramli†||, M El-Metoui†||, M S G Al-Ahmadi†¶, A F Labadz†*, C A Bates†, J L Dunn† and W Ulrici§

† LPMC, Physique 4, Université Blaise Pascal–Clermont Ferrand II, 63177 Aubière Cédex, France

‡ Physics Department, University of Nottingham, Nottingham NG7 2RD, UK

§ Paul-Drude-Institut für Festkörperelektronik, Hausvogteiplatz 5–7, 10117 Berlin, Federal Republic of Germany

Received 1 October 1992, in final form 8 July 1993

Abstract. Non-conventional spectroscopy techniques, in which the electron paramagnetic resonance (EPR) and optical absorption (OA) spectra are thermally detected (TD) via a carbon thermometer at liquid- 4 helium temperatures, are used to investigate the GaP:V system in n-type samples. New TD-EPR results are described. The presence of most of the TD-EPR lines appears to correlate with that of the V^{2+} TD-OA signal. A comparison of the photo-induced effects on the TD-OA V^{3+} and V^{2+} spectra and on the TD-EPR lines is made in order to help in the identification of the latter. A set of resonances in TD-EPR is attributed to a V^{2+} (II) centre, with a 4T_1 ground state, similar to that seen in GaAs:V. A trigonal model where V^{2+} (II) is part of a complex in which one of the neighbouring P ions is replaced by a defect is used to fit the experimental data. Further TD-EPR lines can be due to another V^{2+} ion having also a 4T_1 ground state but which appears to be different from V^{2+} (II).

1. Introduction

Vanadium in III–V materials has been a subject of great interest during the last ten years, particularly in GaAs. However, the GaP:V system is also important, especially from a fundamental point of view for comparison with GaAs:V. The three charges states V^{2+} , V^{3+} and V^{4+} are detected in GaP, while only V^{2+} and V^{3+} are observed in GaAs by optical spectroscopy. The determination of the exact nature of the ground state of the isolated substitutional V^{2+} ion ('isolated' means that the ion is not part of a complex) has been the aim of many studies and discussions. According to Hund's rule the V^{2+} ground state is expected to be 4T_1 whereas Caldas *et al* (1986) predicted a 2E ground state in both GaAs and GaP from theoretical studies. Unfortunately it has not been possible to resolve the problem by experiment, as no conventional electron paramagnetic resonance (EPR) signal that can be attributed to this ion has been detected so far in either GaAs or GaP.

|| Unité de Recherche Associée au Centre National de la Recherche Scientifique No 796.

¶ Now at: Department of Physics, Faculty of Science, King Abdullaziz University, Jeddah, Saudi Arabia.

* Now at: Manchester Computing Centre, University of Manchester, Oxford Road, Manchester M13 9PL, UK.

Experiments have been carried out on the GaAs:V and GaP:V systems using thermally detected (TD) absorption spectroscopy techniques: electron paramagnetic resonance in the microwave range (TD-EPR) and optical absorption in the optical range (TD-OA). TD-EPR has enabled us to observe, in GaAs samples doped with vanadium, two types of spectra attributed to V^{2+} centres: one has been interpreted as being part of a complex and labelled as $V^{2+}(\text{II})$ with a 4T_1 ground state in Vasson *et al* (1992); and the other has been identified very recently as a 2E V^{2+} ion by Vasson *et al* (1993). Taking into account the TD-EPR data and other results in the literature, it was suggested that the latter can be due to the isolated V^{2+} ion. It must be noted that, in GaAs, Görger *et al* (1988) have observed a line they attribute to a V^{2+} centre by optically detected magnetic resonance (ODMR). It is similar to one of the $V^{2+}(\text{II})$ TD-EPR resonances seen at 35 GHz (Vasson *et al* 1992). Resonances similar to those of $V^{2+}(\text{II})$ have also been obtained by TD-EPR in two n-type GaP:V specimens. The first results on $V^{2+}(\text{II})$ in both GaAs and GaP were reported in Vasson *et al* (1984).

The main theme of this paper concerns V^{2+} in GaP. It is based on a TD-EPR study. However, before deciding definitively if the resonances are due to isolated or associated V^{2+} ions, it is necessary to determine if some correlations can be found between the OA signals and the TD-EPR lines in n-type GaP:V samples. In the GaAs:V case, V^{3+} was easily detected by TD-EPR at 35 GHz, so that a comparison of the behaviour of the resonances attributed to V^{2+} centres with that due to V^{3+} was sufficient. However, as V^{3+} is difficult to see by TD-EPR in GaP, TD-OA studies have also been performed. These investigations have given us the opportunity to obtain further OA vanadium-related data, so that the current knowledge concerning V^{3+} and V^{2+} is given first of all. The preliminary data obtained on $V^{2+}(\text{II})$ in GaP (Vasson *et al* 1984) are also summarized. This is followed by some details concerning the spectrometers and on the GaP:V samples that are used in these investigations. Afterwards, new results obtained from TD-EPR studies at X and Q bands are described. The photo-induced effects observed on the TD-OA and the TD-EPR signals in a high-resistivity specimen are then presented and analysed. From a comparison with the GaAs: $V^{2+}(\text{II})$ system, a trigonal model is proposed instead of the orthorhombic model suggested in Vasson *et al* (1984). Finally, the paper concludes with a discussion of the different results, particularly those concerning the V^{2+} centre seen by TD-EPR and also the V^{3+} and V^{2+} OA signals, which have not been reported previously.

2. Background

The vanadium acceptor level in GaP has been measured at $E_c - 0.8$ eV by Clerjaud *et al* (1985) and at $E_c - 0.58$ eV by Ulrici *et al* (1987). It is thus deeper in GaP than it is in GaAs. Table 1 summarizes the signals and corresponding transitions for the different isolated vanadium charge states detected by conventional OA, photoluminescence (PL) and conventional EPR.

2.1. The isolated V^{3+} ion

V^{3+} was the first vanadium ion observed by OA (the 1.2 and 1.75 eV bands; Abagyan *et al* 1974) and PL (zero-phonon lines at 0.79 eV; Kaufmann *et al* 1982). However, these signals were only identified later as due to V^{3+} intracentre transitions from the analyses of Zeeman experiments (Skolnick *et al* 1983, Aszodi and Kaufmann 1985) and analogies in the results given by the three systems InP:V, GaAs:V and GaP:V. Further OA investigations by Clerjaud *et al* (1985) and Ulrici *et al* (1987) have also identified the zero-phonon lines (ZPL) associated with the 1.2 eV (${}^3A_2(\text{F}) \rightarrow {}^3T_1(\text{F})$) and 1.75 eV (${}^3A_2(\text{F}) \rightarrow {}^3T_1(\text{P})$) bands in

Table 1. Summary of the spectroscopic investigations by conventional techniques on isolated V^{3+} and V^{2+} in GaP.

Ion	Technique	Signal (eV)		Transition
V^{3+}	OA	Band ~ 1.2	(a)	${}^3A_2 \rightarrow {}^3T_1(F)$
		Band ~ 1.2	(b),(c)	
		ZPL 1.0782	(b),(c)	
		ZPL 1.0800	(b),(c)	
		ZPL 1.0861	(b),(c)	
		Band ~ 1.75	(a)	${}^3A_2 \rightarrow {}^3T_1(P)$
		Band ~ 1.75	(d)	
		ZPL 1.720	(d)	
		ZPL 1.722	(d)	
		ZPL 1.729	(d)	
	ZPL 0.7912	(b)	${}^3A_2 \rightarrow {}^3T_2(F)$	
	ZPL 0.7931	(b)		
	ZPL 0.7933	(b)		
	Band ~ 0.85	(a)		
	PL	Band ~ 0.76	(d)	${}^2T_2(F) \rightarrow {}^3A_2$
ZPL 0.791		(e)		
ZPL 0.793		(e)		
EPR		(f)	Within 3A_2	
V^{2+}	OA	Band ~ 1	(b),(c)	${}^4T_1(F) \rightarrow {}^4T_1(F)$ or $\rightarrow {}^4A_2(F)$
		Band ~ 1	(b),(c)	

Key: (a) Abagyan *et al* (1974); (b) Clerjaud *et al* (1985); (c) Ulrici *et al* (1987); (d) Kaufmann *et al* (1982); (e) Aszodi and Kaufmann (1985); (f) Kreissl and Ulrici (1986).

addition to those seen in PL (${}^3A_2(F) \rightarrow {}^3T_2(F)$). A theoretical study of the ${}^3A_2(F) \rightarrow {}^3T_1(F)$ transition has been made by Dunn *et al* (1990) and Badran (1991). Also, Kreissl and Ulrici (1986) have identified V^{3+} by conventional EPR. Some years previously, Masterov *et al* (1978) had assigned a conventional EPR signal to a V^{3+} centre. However, this particular signal is unlikely to be due to the isolated V^{3+} ion because the spectrum displays axial symmetry.

2.2. The isolated V^{2+} ion

In strongly n-type GaP:V samples, Clerjaud *et al* (1985) and Ulrici *et al* (1987) found an OA band, close to 1 eV, which was interpreted as due to the isolated V^{2+} by the first authors. Also in GaP, the thermal conductivity experiments of Sahraoui-Tahar *et al* (1989) have shown strong phonon scattering, which was attributed by these authors to the isolated V^{2+} ion with a 4T_1 rather than a 2E ground state.

2.3. Previous TD-EPR results on $V^{2+}(II)$

Preliminary results obtained by TD-EPR on n-type vanadium-doped GaP samples from Wacker Chemitronic were reported in Vasson *et al* (1984). The experiments were carried out at X band with magnetic fields up to 0.6 T. Spectra exhibiting many intense lines were

observed. From the analysis of the dependences of the resonance fields on the microwave frequency ν , varying between 8.0 and 12.4 GHz, for particular orientations of the sample in the magnetic field, three zero-field splittings (ZFS) equal to 4.5, 12.2 and 16.7 GHz (one being the sum of the other two) were determined. The centre responsible was identified as a V^{2+} ion having a 4T_1 ground state with three Kramer doublets as lowest levels. Similar results were reported for GaAs:V. An orthorhombic site for this V^{2+} centre was suggested for both systems. In GaAs, a model with orthorhombic random strains was then considered first of all (En-Naqadi *et al* 1988). However, a 'trigonal' model in which the V^{2+} ion is associated with a defect at an As near-neighbour site is preferred now (Vasson *et al* 1992). This V^{2+} centre is denoted by $V^{2+}(\text{II})$. We shall also use this label for the centre responsible for the intense resonance in GaP:V corresponding to the three ZFS indicated above. The $V^{2+}(\text{II})$ lines in both GaAs and GaP are mainly RF (radiofrequency) electric-field-induced. The same lines have also been observed by acoustically detected (AD) EPR (Vasson *et al* 1986).

3. Experimental details

In our TD absorption spectroscopy techniques, the temperature rise of the sample, due to spin-lattice relaxation or non-radiative de-excitation, which follows the absorption, is detected via a carbon or germanium thermometer at liquid-helium temperatures. In the cells used for the TD-EPR and TD-OA experiments described here, the sample-holder-thermometer assemblies are very similar. A sapphire (pure alumina single crystal) or quartz rod is both the sample holder and the thermal connector between the sample and a carbon-glass thermometer, so that the latter can be positioned outside the microwave resonator or the light path.

The TD-EPR experiments have been carried out between 8.0 and 12.4 GHz and also at 34.85 GHz with a static magnetic field varied from 0 to 3 T. The resonator is an X band waveguide portion in both the X and Q frequency ranges. The sample can be illuminated during the measurements via optical fibres in order to observe the photo-induced effects on the TD-EPR signals. The TD-OA spectrometer is similar to that described in Nakib *et al* (1988) but with a higher resolution. The spectra are obtained between 2 and 5 K in TD-EPR, depending upon the heating of the sample by the microwaves, and at a temperature close to 1.8 K in TD-OA.

Different n-type GaP samples doped only with vanadium or co-doped with sulphur (V:S) have been investigated. Information on the samples used is summarized in table 2. The specimens have been characterized using TD-OA. The spectra obviously depend upon the type of the specimen and on the Fermi-level position. The presence of the V^{3+} and/or V^{2+} signals is also indicated in table 2.

Before illumination, the spectrum of the semi-insulating (SI) sample E1 of GaP:V exhibits the bands and associated ZPL corresponding to the $^3A_2 \rightarrow ^3T_1(\text{F})$ and the $^3A_2 \rightarrow ^3T_1(\text{P})$ transitions within the V^{3+} ion. (The triple-peaked band and ZPL due to the former can be seen later in figure 5.) The spectra of GaP:V (sample Wa18) and of the samples co-doped with sulphur having smaller values of resistivity are dominated by the 1.0 eV band attributed to V^{2+} . For GaP:V (sample Wa17), the V^{2+} and V^{3+} TD-OA signals are seen together. (The V^{2+} spectrum in sample Wa18 is also included later in figure 5.) It must be noted that a small structure with sharp lines at 1.091 and 1.097 eV is superimposed on the V^{2+} band. It is particularly clear in the GaP:V:S samples and it is very similar to the V^{3+} ZPL. However, a small energy shift is observed. This result has not yet been interpreted.

Table 2. Label and vanadium concentration of the investigated samples: (a) sample from the Zentralinstitut für Elektronenphysik; (b) sample from Wacker Chemitronic; si \equiv semi-insulating and sc \equiv semiconducting. The samples labelled 'E' are cut from the tail of a boule, and samples 'A' are from the seed part of the boule. The concentrations of sulphur in GaP:V:S (samples E1 and A1) are 14.5×10^{16} and $43 \times 10^{16} \text{ cm}^{-3}$ respectively. Samples Wa17 and Wa18 also contain sulphur (Kaufmann *et al* 1982). Indications of the presence of the V-related signals observed by TD-OA and TD-EPR are also given for each sample.

Sample		Vanadium concentration (cm^{-3})	TD-OA		TD-EPR $\text{V}^{2+}(\text{II})$
			V^{3+}	V^{2+}	
GaP:V E1	si(a)	7×10^{16}	X	*	*
GaP:V Wa17	sc(b)	3.3×10^{16}	X	X	X
GaP:V Wa18	sc(b)	—		X	X
GaP:V:S E1-E1/2	sc(a)	7×10^{16}		X	X
GaP:V:S A1-A1/2	sc(a)	1.52×10^{16}		X	X

Key: X \equiv a strong or medium strength signal; * \equiv signal created by illumination.

4. TD-EPR studies: the $\text{V}^{2+}(\text{II})$ centre

New TD-EPR experiments have been carried out at X band, with magnetic fields up to 3 T, and at Q band. Some results will be reported here.

4.1. Experimental studies at X band for magnetic fields up to 3 T

All the n-type samples investigated exhibit the $\text{V}^{2+}(\text{II})$ spectrum. As in the case of GaAs, the $\text{V}^{2+}(\text{II})$ resonances are seen in the 'as-received' semiconducting (sc) specimens but they only appear after illumination in the si crystal. It must be noted that the latter has not been studied previously by TD-EPR; Vasson *et al* (1984) made measurements on samples Wa17 and Wa18 below 0.56 T only. Figure 1 shows a typical TD-EPR spectrum obtained in GaP:V (sample Wa17) at 8.75 GHz, when the magnetic field, B , is parallel to the [00 1] axis. The frequency (ν) dependences of the resonance fields have been measured for fields up to 3 T. The experimental results are plotted in figure 2 for GaP:V (sample Wa17) when B is along the [00 1] axis. As observed previously (Vasson *et al* 1984), many of the points can be connected by straight lines. Those lines having negative slopes and intercepting the ν axis at 12.2 and 16.7 GHz are found again, together with other points leading to the third ZFS at 4.5 GHz. However, further resonances that also lie on straight lines with negative slopes have been obtained. Assuming a linear dependence of resonant field on ν , another ZFS of 41.3 GHz is obtained from resonances above 1 T.

Isofrequency curves have been drawn for different values of ν at X band, when B is rotated in the (1 $\bar{1}$ 0) and (00 1) planes. However, none of them exhibits an identifiable symmetry.

It must also be noted that an S-related signal is observed in Wacker samples (which also contain sulphur) and in crystals co-doped with sulphur. In the latter and in sample Wa18, a negative resonance, associated with S and similar to that seen in GaP:S specimens by TD-EPR, is observed. It is in good agreement with the EPR results of Muller *et al* (1989), at frequencies between 140 and 560 GHz, and with those in our laboratory between 35 and 67 GHz obtained using a low-temperature bolometer as a detector. The negative signal is interpreted in terms of a Fano effect (Fano 1961, Muller *et al* 1989).

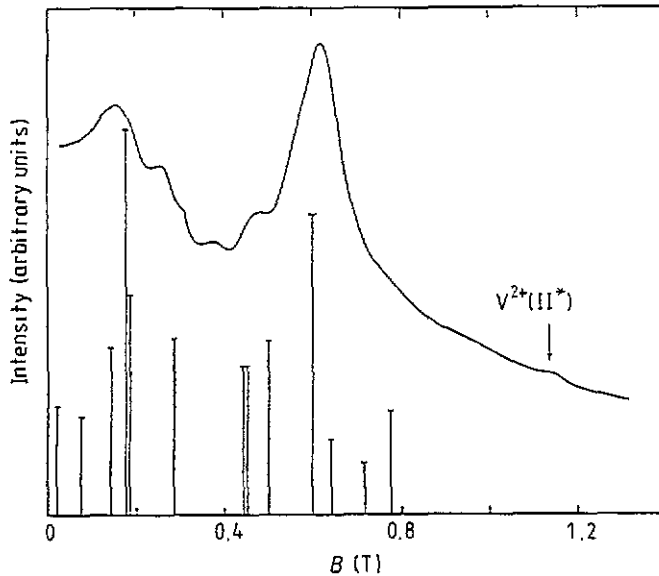


Figure 1. The TD-EPR spectrum at 8.75 GHz in GaP:V (sample Wa17) for B along the [001] axis. The intensities of the predicted peaks for a trigonal $V^{2+}(\text{II})$ centre (with ZFS 4.5, 12.2 and 16.7 GHz) are also indicated for comparison. The resonance at 1.15 T is attributable to a V^{2+} ion having an energy level separation equal to 41.3 GHz ($V^{2+}(\text{II}^*)$).

4.2. Experimental studies at Q band

The GaP:V samples E1, Wa17 and Wa18 have been investigated at 35.85 GHz. Figure 3 shows the TD-EPR spectra in sample E1 before and after illumination and in sample Wa17 in the 'as-received' state for different values of the angle θ between B and the [001] axis, B being in the $(1\bar{1}0)$ plane. For all orientations, many intense overlapping resonances are observed below 1.5 T. Above this value of field, only weak signals have been seen. The intensities of the lines appear to vary with the sample. This is mainly due to the different geometries of the crystals in the RF fields in the two experiments. Sample Wa18 exhibits similar spectra on which is superimposed the sharp negative resonance attributed to sulphur in the $g = 2$ region. An experimental isofrequency diagram is presented in figure 4 for B rotated in the $(1\bar{1}0)$ plane.

Before choosing a model for the V^{2+} centres responsible for these TD-EPR results, some comments can be made.

- (i) The TD-EPR lines are really vanadium-related (obtained in all n-type GaP samples doped with vanadium and only in these samples).
- (ii) Their presence corresponds to that of the isolated V^{2+} TD-OA signal (table 2).
- (iii) Their intensities can be affected by light (lines created by light in E1 and amplified in Wa17) so that the illumination effects on the TD-EPR lines and on the V^{3+} and V^{2+} TD-OA signals can be compared.

5. Photo-induced effects in TD-OA and TD-EPR

As only the semi-insulating E1 sample of GaP:V exhibits important photo-induced effects in both TD-OA and TD-EPR, we shall concentrate on that sample.

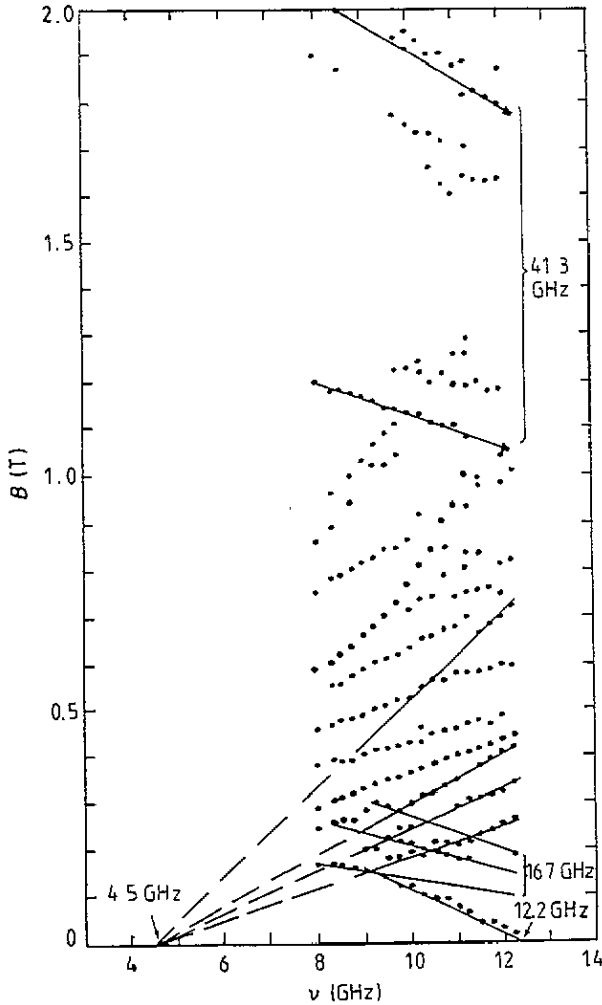


Figure 2. The frequency dependences of the positions of the TD-EPR peaks in GaP:V (sample Wa17) for B along the $[001]$ axis, at X band.

5.1. TD-OA experiments

As stated previously, the TD-OA spectrum of this sample, cooled in the dark and before illumination, exhibits several bands and lines. These include the V^{3+} signals and further new lines, which have still to be identified. The latter, labelled as X and Y in figure 5, appear at energies 1.35 and 1.31 eV respectively. They are observed on the high-energy side of the ${}^3A_2(F) \rightarrow {}^3T_1(F)$ band of V^{3+} . After illumination with light of increasing energy (above 1.25 eV), a decrease of the intensities of the V^{3+} bands and ZPL, and also of the X and Y lines, is observed. At the same time, the band attributed to the isolated V^{2+} ion by Clerjaud *et al* (1985) appears together with an unidentified signal labelled Z. V^{4+} is also seen after illumination (figure 5). The decay times of the photo-induced effects are equal for the V^{3+} and V^{2+} signals, in agreement with their identification.

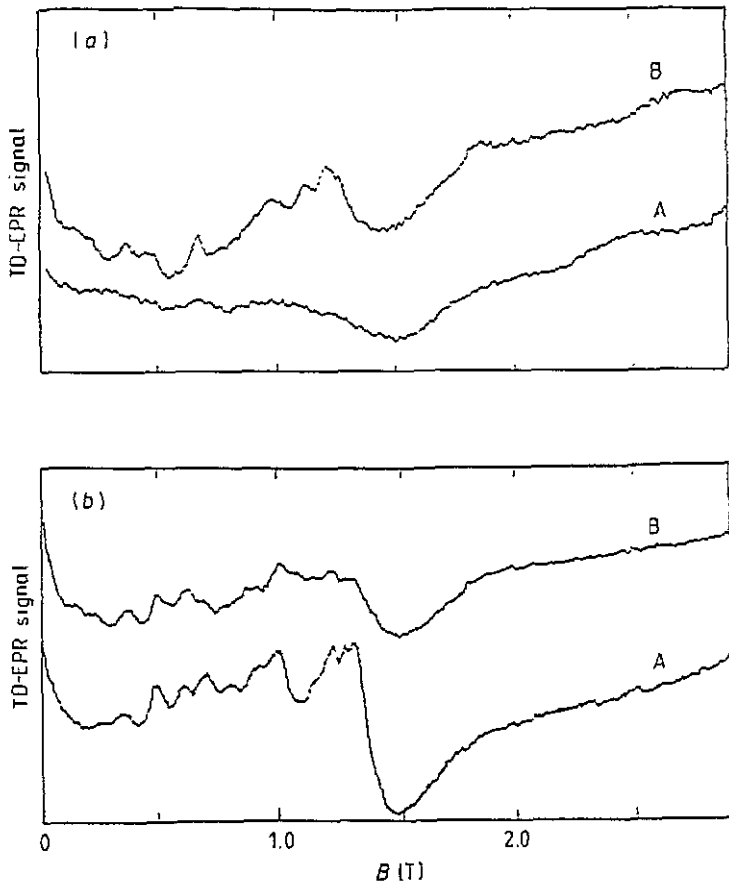


Figure 3. The TD-EPR spectra at 34.85 GHz in GaP:V. (a) Sample E1 before illumination (A) and after illumination with light of energy $h\nu_{\text{exc}} = 2.07$ eV (B) for $\theta = 65^\circ$. (b) Sample E1 after illumination (A) and sample Wa17 as received (B) for B along the $[1\ 1\ 0]$ axis for $\theta = 90^\circ$.

5.2. TD-EPR experiments

The photo-induced effects have been investigated at both X and Q bands. The E1 sample has been illuminated through optical fibres using a halogen lamp and different interference filters. The TD-EPR lines created are persistent after illumination.

5.3. Comparison of the spectral dependences of the TD-EPR signals and their interpretation

The amplitudes of the TD-OA and TD-EPR signals have been measured as functions of the illumination photon energy $h\nu_{\text{exc}}$. The spectral dependences obtained are shown in figure 6; the TD-OA results are given for the isolated V^{3+} and V^{2+} ions in figure 6(a) and the lines labelled as X, Y and Z in figure 6(b). For comparison, figure 6(c) displays the TD-EPR lines that appear after illumination and which can be related to $V^{2+}(\text{II})$. All lines have a first onset at $h\nu_{\text{exc}} = 1.25$ eV. A second onset is seen for isolated V^{3+} and V^{2+} and for Y, Z and $V^{2+}(\text{II})$ at 1.75 eV. However, the amplitude of line X decreases sharply to zero above 1.25 eV and then does not exhibit the 1.75 eV onset, so that its behaviour is different from the other lines.

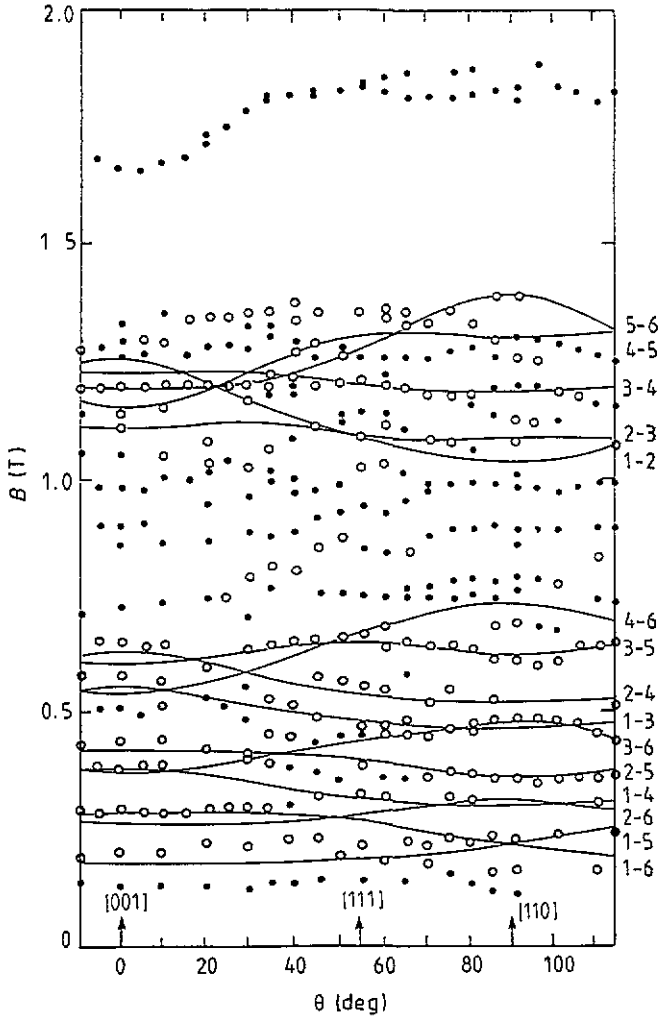


Figure 4. The experimental isofrequency diagrams obtained from samples E1 and Wa17 of GaP:V at 34.85 GHz, for B rotated in the $(1\bar{1}0)$ plane. Full and open circles are experimental points (samples E1 and Wa17). The curves indicated by open circles fit the curves calculated for $V^{2+}(\text{II})$ using the spin Hamiltonian trigonal model with $S = 5/2$ in the zero-strain approximation. The theoretical curves calculated for sites 2 and 3 with this model are indicated by full curves. The transitions are indicated by the numbers 1, 2, ..., 6 of the levels involved, 1 being the level of lowest energy and 6 the highest.

The decrease of the TD-OA signal of V^{3+} correlates well with the increase in the signal from V^{2+} . It is in good agreement with the increase of the amplitudes of Z and of the $V^{2+}(\text{II})$ TD-EPR lines. The spectral dependence of Y is very close to that of V^{3+} .

Sample E1 of GaP:V is semi-insulating with its Fermi level pinned by an energy level near to the middle of the gap. The latter could be the $P_{\text{Ga}}^{4+}/P_{\text{Ga}}^{5+}$ level. Using conventional EPR, Kreissl and Ulrici (1986) have observed the P_{Ga}^{4+} and V^{3+} resonances and their photo-induced changes in a sample cut from the same part of the same boule as the specimen

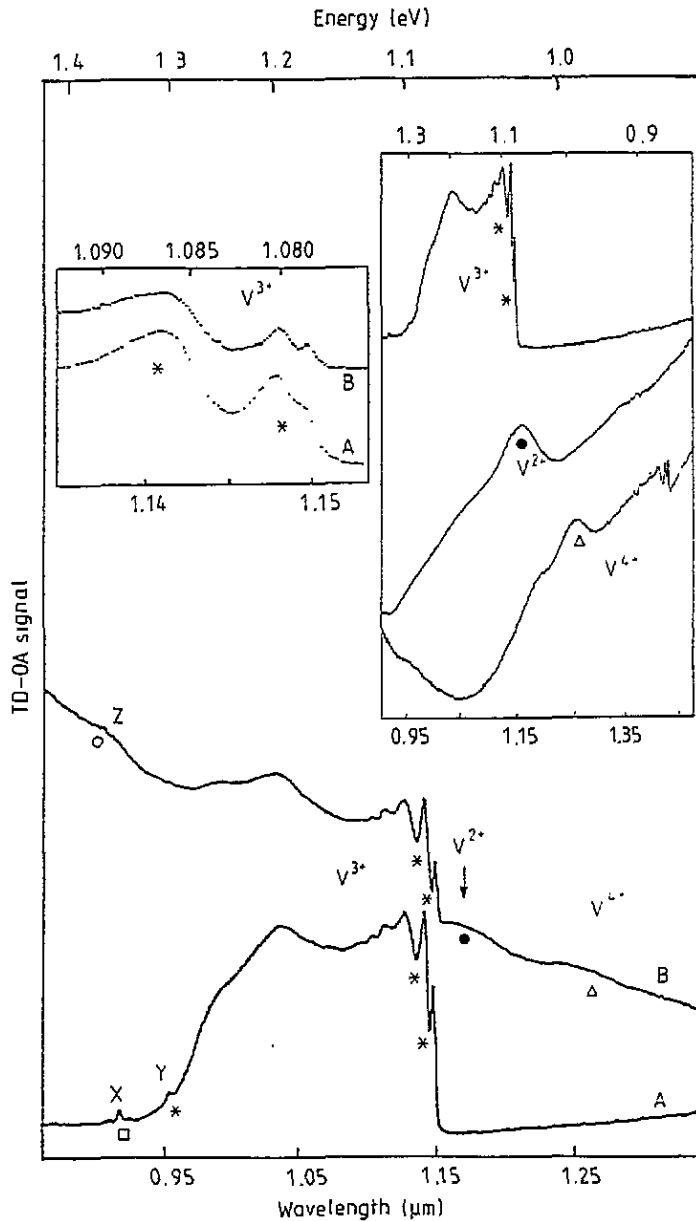


Figure 5. The TD-OA spectra from sample E1 of GaP:V before illumination (A) and after illumination with light of energy $h\nu_{exc} = 2.3$ eV (B), showing the decrease of the V^{3+} band and ZPL together with the creation of the V^{2+} and V^{4+} signals after illumination. Details of the V^{3+} ZPL are given in one of the inserts. The other insert shows the positions of the nearly pure V^{3+} , V^{2+} and V^{4+} signals in the 1.1 eV region (sample E1, Wa18 and p-type GaP:V samples respectively) for comparison.

studied here. From this, the photo-induced recharging processes occurring above the 1.25 eV onset should be:

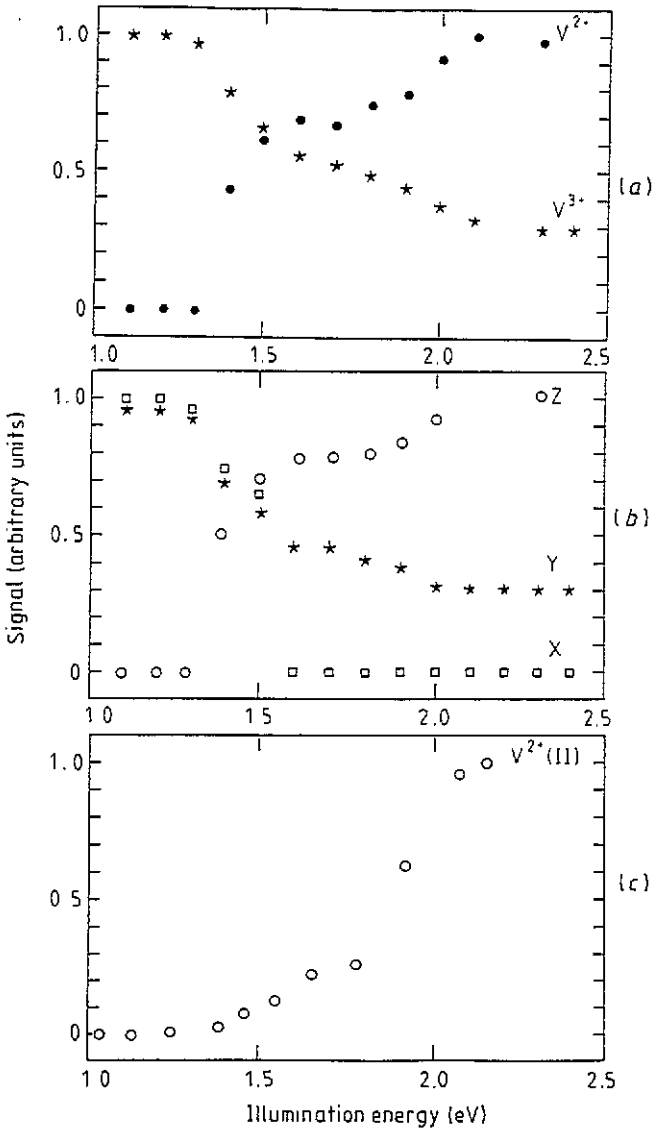
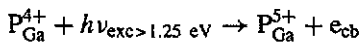


Figure 6. The dependences of the photo-induced changes of the TD signals on the energy of illumination in sample GaP:V E1: (a) TD-OA signals of V^{3+} (*) and V^{2+} (●); (b) further TD-OA lines X (□), Y (*) and Z (○); (c) TD-EPR signal attributed to $V^{2+}(II)$ (○).



where e_{cb} denotes an electron in the conduction band.

The second onset is in good agreement with the energy difference between the isolated V^{2+}/V^{3+} level and the top of the valence band found by Ulrici *et al* (1987). The behaviour of the V^{3+} and V^{2+} TD-OA spectra can be interpreted by the relation:

$$V^{3+} + h\nu_{\text{exc} > 1.75 \text{ eV}} \rightarrow V^{2+} + h\nu_b$$

where $h\nu_b$ denotes a hole in the valence band. The spectral dependence of $V^{2+}(\text{II})$ indicates that it can be isolated. However, if it is *not* isolated, the results suggest that the type II vanadium acceptor level is close to that of the isolated vanadium and that

$$V^{3+}(\text{II}) + h\nu_{\text{exc} > 1.75 \text{ eV}} \rightarrow V^{2+}(\text{II}) + h\nu_b.$$

The creation of the V^{4+} TD-OA signal can then be due to the capture of a hole by V^{3+} .

6. The trigonal model for $V^{2+}(\text{II})$

Taking into account the similarity between the behaviour of $V^{2+}(\text{II})$ in both GaAs and GaP, the trigonal model developed for GaAs, where $V^{2+}(\text{II})$ is associated with a near-neighbouring defect (Vasson *et al* 1992), will be tested in the GaP: $V^{2+}(\text{II})$ case.

The TD-EPR lines detected at X band in n-type GaP samples containing vanadium give rise to three small ZFS similar to those found in GaAs:V. They can be interpreted in terms of a $V^{2+}(\text{II})$ centre with a 4T_1 ground state. A further ZFS of 41.3 GHz is obtained in GaP. The question arises: 'Does it also correspond to $V^{2+}(\text{II})$ or to another V^{2+} centre?'

In Vasson *et al* (1992) we concluded that $V^{2+}(\text{II})$ in GaAs could be a V^{2+} ion associated with a defect replacing a near-neighbour As atom and creating a trigonal field at the V^{2+} site. Reasonable agreement was obtained between the theoretical and experimental results. Consequently we will use the same trigonal model here for GaP: $V^{2+}(\text{II})$ with the associated defect occupying a P site.

The ground state of a $V^{2+}(\text{II})$ ion, which remains a 4T_1 state after the consideration of the Jahn–Teller (JT) effect, is split into six Kramers doublets by the spin–orbit coupling and the trigonal field, assuming both to be of the same order of magnitude. We further assume that only the three smallest ZFS found in the experiments originate from GaP: $V^{2+}(\text{II})$ and correspond to the spacings of the three Kramers doublets of lowest energies. The other three doublets are sufficiently high in energy (ignoring the 41.3 GHz splitting) that they can be omitted in this analysis. The lowest doublets can then be described by a spin Hamiltonian, with an effective spin $S = 5/2$, of the form

$$\mathcal{H}_{\text{spin}} = \mathcal{H}_A + \mathcal{H}_B + \mathcal{H}_D + \mathcal{H}_{\text{trig}} \quad (6.1)$$

where \mathcal{H}_A is the cubic term describing the spin–orbit coupling (in fourth order), \mathcal{H}_B is the Zeeman term and \mathcal{H}_D describes the random strain of E symmetry. All of these contributions to the spin Hamiltonian are the same for all four trigonal sites and are given by the following (Vasson *et al* 1992):

$$\begin{aligned} \mathcal{H} &= A[S_x^4 + S_y^4 + S_z^4 - \frac{1}{5}S(S+1)(3S^2 + 3S - 1)] \\ \mathcal{H}_B &= g\mu_B \mathbf{B} \cdot \mathbf{S} \\ \mathcal{H}_D &= D[3S_z^2 - S(S+1)] \end{aligned} \quad (6.2)$$

where A , g and D are respectively the cubic, g -value and strain parameters and Oz is a twofold axis of the tetrahedral cluster. The trigonal fields differ for each of the four sites. However, they can be written in the consolidated form:

$$\mathcal{H}_{\text{trig}} = \alpha' \mathcal{H}_X + \alpha'' \mathcal{H}_Y + \alpha''' \mathcal{H}_Z \quad (6.3)$$

Table 3. The values of D obtained for the $V^{2+}(\text{II})$ TD-EPR peaks at a frequency of 8.75 GHz for the transitions indicated (labelled by the energies of the levels at the stated magnetic field with '1' as the lowest). Also given is the corresponding direction of B (along x or z) and its magnitude. Intensities less than 1.0 have been excluded from the table.

B (T)	Transition	D (GHz)	Intensity (arbitrary units)
0.018	4-6 x	-0.57	2.39
0.076	2-4 z	-0.81	2.12
0.143	1-3 z	-0.02	3.68
0.177	1-3 x	-0.41	8.38
0.181	2-4 x	0.29	4.83
0.284	2-3 x	-1.08	3.87
0.445	1-2 x	-0.70	3.26
0.455	1-2 z	0.36	3.26
0.509	3-4 x	-0.12	3.81
0.600	2-3 z	0.55	6.54
0.640	5-6 z	-2.30	1.65
0.716	3-4 z	-1.48	1.12
0.777	5-6 z	-0.72	1.78

where

$$\mathcal{H}_X = E(S_y S_z + S_z S_y) \quad (6.4)$$

with cyclic interchanges for \mathcal{H}_Y and \mathcal{H}_Z , and where the parameters α' , α'' and α''' take the value unity with the respective signs:

- + , + , + for sites 1 corresponding to the trigonal direction $[1\ 1\ 1]$
- + , - , - for sites 2 corresponding to the trigonal direction $[1\ \bar{1}\ \bar{1}]$
- , + , - for sites 3 corresponding to the trigonal direction $[\bar{1}\ 1\ \bar{1}]$
- , - , + for sites 4 corresponding to the trigonal direction $[\bar{1}\ \bar{1}\ 1]$.

Using the first procedure adopted in Vasson *et al* (1992) for the case of the X-band results, we have tried to predict the peak positions in calculating their maximum intensities, assuming that the transitions are mainly RF electric-field-induced, as observed experimentally. Values of E , A and D were first calculated from ZFS. We obtain

$$E = +0.90 \pm 0.05 \text{ GHz}$$

$$A = -0.18 \pm 0.07 \text{ GHz}$$

for D varying between -0.31 and $+0.35$ GHz. The value of g was then deduced from the B versus ν laws using g in the range 1.0 to 2.9. The best fit is given by $g_{\parallel} = g_{\perp} = 1.40 \pm 0.05$. It must be remembered that this g -factor is an effective g , which contains the real (strain-independent) g and a part coming from a strain-dependent term included in $g\mu_B \mathbf{B} \cdot \mathbf{S}$.

The maximum intensities have been calculated with these values of E , A , g_{\parallel} and g_{\perp} for each transition and for the different frequencies investigated at X band, when B is along the $[001]$ axis. As observed for GaAs: $V^{2+}(\text{II})$, the strain parameter D varies from one transition to the other and with the frequency. The intensities of different transitions are indicated in the spectrum drawn in figure 1, at 8.75 GHz. Their values are given in table 3 together with the positions of the peaks and the values of the strains (which are small). No line is expected above 0.8 T for this particular frequency, in agreement with the location of the most intense lines, which are all observed below 0.8 T. The resonance seen at about 1.15 T corresponds to the ZFS at 41.3 GHz, which is not considered in this analysis.

A second procedure was used in Vasson *et al* (1992) for the fit to the Q-band results. In this case, as the change in the energy due to the strains is a smaller fraction of the microwave quantum than it is at X band, the strains are neglected. Isofrequency curves have been calculated in such a condition. For GaP:V²⁺(II), we obtain the best fit to experimental curves by taking $g_{\parallel} = g_{\perp} = 2.07$, as in the case of GaAs:V²⁺(II), with $E = +1.21$ GHz and $A = -0.20$ GHz. It is not possible to present all the theoretical isofrequency curves for the four sites of V²⁺(II) together with the experimental diagrams because of the resulting complexity. However, the experimental points plotted in figure 4 that fit the theoretical curves are indicated by open circles. This figure also shows the isofrequency diagrams calculated for sites 2 and 3, which are equivalent, for B rotated in the (110) plane. As in the case of GaAs:V²⁺(II), a reasonable fit is obtained.

We have also considered the possibility that the fourth ZFS of 41.3 GHz also belongs to the V²⁺(II) energy level scheme. With such an assumption, the V²⁺(II) centre has four closely spaced lowest Kramers doublets, which can be described using a spin Hamiltonian with an effective spin of $S = 7/2$. The isofrequency curves have been recalculated under these assumptions. However, it has not been possible to find a satisfactory fit to the experimental data and thus it appears that the 41.3 GHz ZFS does not belong to V²⁺(II). One of these lines corresponding to this ZFS of 41.3 GHz can be seen very clearly in figure 1 (labelled as V²⁺(II*)).

7. Discussion

For V²⁺, two important problems must be solved.

- (i) What is the nature of the ground state of the isolated V²⁺ ion in GaP? Is it ⁴T₁ or ²E, and is it the same as that of the isolated V²⁺ ion in GaAs?
- (ii) Is the V²⁺ centre, labelled as V²⁺(II) and responsible for the intense TD-EPR lines, seen in n-type samples, isolated or part of a complex?

We have a number of points to make before attempting to find answers to these two fundamental questions. First, as with the GaAs:V system, n-type crystals of GaP containing vanadium exhibit a set of many lines, which *either* appear after illumination in the SI sample *or* are present in the as-received state (but which can be slightly amplified or not affected by the illumination, depending on the resistivity). Secondly, from all our results, it is clear that the centre (or centres) responsible for these spectra is (or are) also divalent vanadium ions having a ⁴T₁ ground state. The centre giving rise to the resonances corresponding to transitions within the three Kramers doublets having ZFS of 4.5, 12.2 (and their sum 16.7) GHz, labelled as V²⁺(II), is the same as the centre labelled as V²⁺(II) in GaAs. However, thirdly, we have seen that, in GaP, frequency-dependence studies at X band lead to a further ZFS of 41.3 GHz.

If we examine all the TD-EPR experimental results, together with the TD-OA data for the GaP:V system, it appears that V²⁺(II) can be isolated. The TD spectra show the simultaneous presence of the V²⁺(II) and isolated V²⁺ centres in SC specimens and generally the creation of their signals, after illumination, in the SI crystal (table 2). In the latter sample, the spectral dependences of the isolated V²⁺ TD-OA spectrum and of the V²⁺(II) TD-EPR lines are similar and also are in agreement with that found for the isolated V³⁺ TD-OA, all having the same onsets. This strongly suggests that these signals relate to the same centre. Furthermore, the value of one of the onsets is in good agreement with the position of the isolated vanadium acceptor level at $E_c - 0.58$ eV. Nevertheless, a discrepancy seems to arise in the decay

times of the photo-induced effects in TD-OA and TD-EPR; 2 h after illumination, the effects on the TD-OA signals of the isolated V^{3+} and V^{2+} have disappeared (in agreement with the observation in conventional OA) while the decrease of the amplitudes of the $V^{2+}(\text{II})$ TD-EPR lines is small. These results would suggest that the two V^{2+} centres are different. However, even if the TD-OA and TD-EPR cells are similar, the probes used in the near-infrared and microwave ranges are very different. This could mean that the extra unwanted infrared radiation to which the sample is subjected can strongly change in the two types of experiments.

We have carried out further TD-OA and TD-EPR measurements together, using the same probe (the one which is used for the TD-EPR experiments) during the same sequences of illuminations. The optical fibres attached to the TD-EPR probe for the illumination of the sample also allow us to perform TD-OA experiments. Under such conditions, we have found that the decay times of the photo-induced effects are the same for the TD-OA signals of the isolated V^{3+} ion (which were sufficiently intense to be detected easily with this arrangement) and for the TD-EPR lines of $V^{2+}(\text{II})$. This result shows that decay times of photo-induced effects can only be compared if the probes are the same. Thus the different decay times observed in TD-OA and TD-EPR experiments are *not* by themselves proof that $V^{2+}(\text{II})$ and isolated V^{2+} are different.

However, on taking into account the obvious similarities between $V^{2+}(\text{II})$ (ground state 4T_1) in GaAs and GaP, it is logical to say that its nature is the same in both materials. In the case of GaAs, we have concluded that $V^{2+}(\text{II})$ is very probably part of a complex (Vasson *et al* 1992) so that, in GaP, $V^{2+}(\text{II})$ can be expected similarly to be a V^{2+} ion at a Ga substitutional site associated with a defect at a nearest-neighbour P site. A very reasonable fit is observed between a series of TD-EPR lines, including the most intense seen in the spectra, which we have attributed to $V^{2+}(\text{II})$, with the calculation using the trigonal model for a spin Hamiltonian with an effective spin $S = 5/2$ if only the three lowest Kramers doublets, which correspond to the three smallest ZFS, are considered. The poor agreement found between experiment and theory using the fourth ZFS suggests that a second V^{2+} centre different from $V^{2+}(\text{II})$ contributes to the TD-EPR spectra. It is labelled as $V^{2+}(\text{II}^*)$. It also has a 4T_1 ground state and its lowest levels are two Kramers doublets separated by 41.3 GHz. It must be remembered that, in GaAs, a second V^{2+} ion has also been detected by TD-EPR. However, its ground state is 2E (Vasson *et al* 1993).

Now we examine our results taking into account data found in the literature. $V^{2+}(\text{II})$ and $V^{2+}(\text{II}^*)$ both have a 4T_1 and not a 2E ground state as predicted by Caldas *et al* (1986). It appears to be very interesting to compare our TD-EPR investigations and the thermal conductivity experiments of Sahraoui-Tahar *et al* (1989). In GaP:V, these authors observed two strong phonon scattering peaks, indicating the presence of two V^{2+} centres each with T_1 ground states. One of these peaks occurs below 1 K and gives 12 GHz for the frequency of the process responsible. This value is in excellent agreement with one of the ZFS obtained by TD-EPR for $V^{2+}(\text{II})$. A similar result was observed for GaAs: $V^{2+}(\text{II})$ by Vasson *et al* (1992) and by Butler *et al* (1989). The only difference in the case of GaP: $V^{2+}(\text{II})$ is that, although the samples investigated by the two techniques were cut from the same part of the same boule, the $V^{2+}(\text{II})$ TD-EPR lines were sensitive to illumination but the 12 GHz phonon scattering peak was present in the dark and unaffected by illumination. However, we have noticed that the photo-induced effects can depend upon the 'history' of the sample taking into account the sequences of the cooling and illumination processes, and that the effects can sometimes remain after the specimen has been heated at room temperature and then cooled again in the dark. We conclude therefore that the 12 GHz phonon scattering can be due to $V^{2+}(\text{II})$.

The second phonon scattering peak in GaP:V is obtained at 7 K and gives a resonant frequency of 380 GHz. It is attributed by Sahraoui-Tahar *et al* (1989) to the 4T_2 - 4T_1 inversion splitting associated with a dynamic orthorhombic JT effect operating within the T_1 ground orbital state of the isolated V^{2+} ion. As in the cases of the isolated V^{2+} TD-OA signal and the $V^{2+}(\Pi^*)$ (and also $V^{2+}(\Pi)$) TD-EPR lines, the 380 GHz peak is created by the illumination. It is worth recalling here that Butler *et al* (1989) have only found weak high-frequency phonon scattering in GaAs:V, indicating, from their studies, a 2E ground state for the isolated V^{2+} ion, and that we have detected a 2E V^{2+} ion in GaAs by TD-EPR (Vasson *et al* 1993).

At this stage, comparing all the TD and phonon scattering results, it seems logical to conclude that $V^{2+}(\Pi)$ is part of a complex even though we are unable to propose a microscopic model for such a centre. Complexes of transition metal (TM_{Ga}) acceptors with shallow donors (trigonal [$TM_{Ga}-S_P$] centres) can be formed, driven by the Coulomb attraction, as has been shown recently by conventional EPR for Fe and Cr in GaP (Kreissl *et al* 1992). It must be noted that the concentration of these complexes amounts to only between 1 and 5% of that of the isolated TM_{Ga} . As $V^{2+}(\Pi)$ is very strongly coupled to the phonons, small concentrations of it can nevertheless be responsible for large TD-EPR signals.

Further questions can arise concerning the isolated V^{2+} ion. Is $V^{2+}(\Pi^*)$ a V^{2+} ion at a site that is subjected to orthorhombic strains and responsible for the high-frequency phonon scattering, and is it isolated? In such a case, the latter has a 4T_1 ground state, which agrees with the intense phonon scattering observed. Thus an orthorhombic model with an effective spin of 3/2 must be used to fit the lines corresponding to transitions between the two Kramers doublets separated by 41.3 GHz. Indeed, such a fit would be expected for an isolated V^{2+} in GaP with a 4T_1 ground state very strongly coupled to the e and t_2 modes of the lattice and very sensitive to orthorhombic strain, as in the case of the isoelectronic Cr^{3+} ion in GaAs (Parker *et al* 1990) or Ni^{2+} in GaP (Erramli *et al* 1991).

In addition, TD-OA signals not previously identified have also been studied. We have seen that the behaviour of the line labelled as Y closely follows that of the bands and of the ZPL of V^{3+} . The decay time of the effects of the illumination is the same for Y and V^{3+} . The centre responsible for Y appears to be a V^{3+} ion and thus the line at 1.31 eV can be interpreted as arising from the ${}^3A_2 \rightarrow {}^1A_1(G)$ transition of the isolated V^{3+} ion. The X line is not due to vanadium. However, the Z band can be attributed to a V^{2+} centre. It is similar to a band seen in GaAs:V by both TD-OA and by magnetic circular dichroism (MCD) and which has also been interpreted as due to a V^{2+} ion (Görger *et al* 1988). From our TD-EPR study (Vasson *et al* 1992) and optically detected magnetic resonance (ODMR) work of Görger *et al* (1988), it would appear to be V^{2+} -related in GaAs.

8. Conclusions

The TD-EPR and TD-OA techniques performed at liquid- 4He temperatures have been particularly useful for the study of the GaP:V system. TD-EPR is extremely sensitive to very strongly coupled ions such as those with T_1 ground states. It has enabled us to detect two types of 4T_1 V^{2+} centres in this material, which have not been observed by conventional EPR. The frequency dependence of the resonances at X band and the experiments at Q band (which are rather easy to carry out because of the possible use of the 3 cm waveguide as the resonator) have been very significant for the study of V^{2+} . Furthermore, by the use of the TD technique we have been able to study the *same* sample in both the microwave and optical frequency ranges, whatever its size (even a large sample can be examined by

TD-EPR at 35 GHz, or a very small sample by TD-OA). This facility is very important for the analysis of photo-induced effects. In addition, TD-EPR and TD-OA may be undertaken using the same probe.

For the two V^{2+} centres detected in GaP, part of the TD-EPR lines are attributed to a ${}^4T_1 V^{2+}$ complex, $V^{2+}(\text{II})$, having three close Kramers doublets as the ground states. The spectra can be interpreted as arising from a V^{2+} ion associated with a defect at a nearest-neighbour P site, which creates a trigonal field. Studies of photo-induced effects of the V-related signals in TD-OA and TD-EPR show that the $V^{2+}(\text{II})/V^{3+}(\text{II})$ and isolated V^{2+}/V^{3+} levels have to be very close in energy and located at $E_v + 1.75$ eV. Also, another set of TD-EPR lines is interpreted as due to another ${}^4T_1 V^{2+}$ ($V^{2+}(\text{II}^*)$) ion with two lowest Kramers doublets separated by 41.3 GHz. Further work must be undertaken in order to confirm whether this centre is the isolated V^{2+} using a Jahn–Teller orthorhombic model as can be expected for such an ion.

From the TD-OA studies, we have furthermore assigned, for the first time, a line to the ${}^3A_2 \rightarrow {}^1A_1(\text{G})$ optical transition of this isolated V^{3+} ion and observed a new band, which can be attributed to a V^{2+} centre. However, it is difficult to be certain about the exact nature of this divalent vanadium.

Acknowledgments

The authors would like to thank Professors L J Challis and B Clerjaud for many long and stimulating discussions on the subject of vanadium in GaAs and GaP. AFL also wishes to thank the SERC for a Research Studentship.

References

- Abagyan S A, Ivanov G A, Kustnetsov Yu N and Okunev Yu A 1974 *Fiz. Tekh. Poluprov.* **8** 1691–6 (Engl. Transl. 1975 *Sov. Phys.–Semicond.* **8** 1096–9)
- Azodi G and Kaufmann U 1985 *Phys. Rev. B* **32** 7108–15
- Badran R I 1991 *PhD Thesis* University of Nottingham
- Butler N, Challis L J, Sahraoui-Tahar M, Salce B and Ulrici W 1989 *J. Phys.: Condens. Matter* **1** 1191–203
- Caldas M J, Figueiredo S K and Fazzio A 1986 *Phys. Rev. B* **33** 7102–9
- Clerjaud B, Naud C, Deveaud B, Lambert B, Plot B, Bremond G, Benjeddou C, Guillot G and Nouailhat A 1985 *J. Appl. Phys.* **58** 4207–15
- Dunn J L, Bates C A and Ulrici W 1990 *J. Phys.: Condens. Matter* **2** 10379–89
- En-Naqadi M, Vasson A, Vasson A-M, Bates C A and Labadz A F 1988 *J. Phys. C: Solid State Phys.* **21** 1137–53
- Erramli A, Al-Ahmedi M S G, Ulrici W, Tebbal N, Kreissl J, Vasson A-M, Vasson A and Bates C A 1991 *J. Phys.: Condens. Matter* **3** 6345–62
- Fano U 1961 *Phys. Rev.* **124** 1866–78
- Görger A, Meyer B K, Spaeth J M and Hennel A M 1988 *Semicond. Sci. Technol.* **3** 832–8
- Kaufmann U, Ennen H, Schneider J, Würmer R, Weber J and Köhl F 1982 *Phys. Rev. B* **25** 5598–606
- Kreissl J and Ulrici W 1986 *Phys. Status Solidi b* **136** K133–7
- Kreissl J, Ulrici W, Rehse U and Gehlhoff W 1992 *Phys. Rev. B* **45** 4113–21
- Masterov V F, Samorukov B E, Sobolevskii V K and Shtel'makh K F 1978 *Fiz. Tekh. Poluprov.* **12** 529–33 (Engl. Transl. 1978 *Sov. Phys.–Semicond.* **12** 305–7)
- Muller F, Brunel L C, Grynberg M, Blinowski J and Martinez G 1989 *Europhys. Lett.* **8** 291–6
- Nakib A, Houbloss S, Vasson A and Vasson A-M 1988 *J. Phys. D: Appl. Phys.* **21** 478–82. Reprinted in *Eng. Opt.* pp 143–7
- Parker L W, Bates C A, Dunn J L, Vasson A and Vasson A-M 1990 *J. Phys.: Condens. Matter* **2** 2841–56
- Sahraoui-Tahar M, Salce B, Challis L J, Butler N, Ulrici W and Cockayne B 1989 *J. Phys.: Condens. Matter* **1** 9313–24

- Skolnick S M, Dean P J, Kane M J, Uihlein C, Rubbins D J, Hayes W, Cockayne B and MacEwan W R 1983 *J. Phys. C: Solid State Phys.* **16** L767-75
- Ulrici W, Eaves L, Friedland K and Halliday D P 1987 *Phys. Status Solidi b* **141** 191-202
- Vasson A, En-Naqadi M and Vasson A-M 1986 *J. Phys. D: Appl. Phys.* **19** 1149-57
- Vasson A, Vasson A-M, Bates C A and Labadz A F 1984 *J. Phys. C: Solid State Phys.* **17** L837-41
- Vasson A-M, Labadz A F, Tebbal N, Vasson A, Gavaix A and Bates C A 1992 *J. Phys.: Condens. Matter* **4** 4565-82
- Vasson A-M, Vasson A, El-Metoui M, Tebbal N and Bates C A 1993 *J. Phys.: Condens. Matter* **5** 2553-60